RSC Advances

Journal Name RSCPublishing

ARTICLE

Effects of Fe Doping on the Strain and Optical Properties of GaN Epilayers Grown on Sapphire Substrates

Cite this: DOI: 10.1039/x0xx00000x

Received 00th January 2012,
Accepted 00th January 2012

DOI: 10.1039/x0xx00000x

www.rsc.org/

C. C. Zheng,[a, b] J. Q. Ning,[b] Z. P. Wu,[b, †] J. F. Wang,[c] D. G. Zhao,[d] K. Xu,[c] J. Gao,[b] and S. J. Xu[b, *]

Abstract Effects of Fe doping were investigated in detail on a series of Fe-doped GaN epilayers with different doping concentrations grown on sapphire substrates by confocal micro-Raman spectroscopy under the back-scattering geometric configuration. Careful investigation of the E_2^{high} and A_1(LO) modes of the Fe- and Si-doped epilayers as well as the intentionally undoped free-standing GaN reveals that the compressive residual strain in the Fe-doped GaN epilayers tends to relax as the Fe concentration increases. This finding is further supported by X-ray diffraction measurements. The relaxation of compressive residual strain is most likely due to the compensation by the tensile strain induced by incorporation of iron atoms in the GaN epilayers. The influence of Fe doping on the background electron concentration was also discussed by analyzing the upper branch of A_1(LO)-plasmon coupled mode.

Introduction

Gallium nitride (GaN) is one kind of technologically important wide bandgap semiconductor due to its tremendous potential for application in different areas, such as light emitting diodes (LEDs), laser diodes, etc.[1, 2] Currently, GaN is usually grown on foreign substrates, such as sapphire, due to the unavailability of a large size GaN substrate. It is well known that intentionally un-doped GaN bulks and thin films always show n-type conductivity. In other words, there is exclusively a background electron gas in the conduction band of even un-doped GaN. Therefore, fabricating semi-insulating and p-type GaN materials is crucial for applying GaN in functional devices.[3-6] Iron (Fe) doping is a promising approach to achieve the semi-insulating and even p-type conductivity in GaN epilayers. On the other hand, residual strain usually exists in such heteroepilayers of GaN and ZnO. Moreover, the residual strain has a strong impact on their optical and electronic properties.[7, 8] In the GaN epilayers grown on sapphire substrates, the residual strain is typically compressive and biaxial in nature.[7] As an effective method of studying lattice vibration and its interaction with carriers, Raman spectroscopy has been adopted widely to investigate strain status in GaN epilayers including Fe-doped epilayers.[9-14] However, a systematic study of the strain, especially evolution of the strain with the Fe doping concentration in GaN epilayers, although highly desirable, does not exist. In this article, we present a detailed study on the effects of Fe doping on the strain and optical properties of the GaN epilayers when the Fe doping concentration varies from 0.013% to 4.7%. Our results clearly demonstrate the partial relaxation of the compressive residual strain and the compensation of Fe dopants to the background electron gas in the GaN epilayers. These findings are interesting and significant for both basic research and practical applications.

Experimental

The GaN epilayers with varying Fe concentrations grown with hydride vapour phase epitaxy (HVPE) on sapphire substrates were adopted in this study. The Fe concentrations were estimated to be 0.013%, 0.16%, 1.6%, 3.1% and 4.7% in the GaN epilayers denoted as F1, F2, F3, F4 and F5, respectively, based on the calibrated growth conditions. Available study has shown that Fe atoms incorporated into GaN have a co-existence charge state of Fe^{2+} and Fe^{3+}.[15] The intentional growth thicknesses of Fe doping layers in samples F1 to F5 were 19, 20, 20, 41 and 97 μm. Before the growth of the Fe doped layers, a 4 μm intentionally undoped GaN buffer layer was deposited. For comparison, an intentionally undoped GaN epilayer (G1) synthesized under the similar conditions and a free-standing GaN bulk (G2) with thickness ~0.3 cm were used as the control samples. In addition, a series of Si-doped GaN epilayers with estimated carrier concentrations of 5.02×10^{15} , 1.52×10^{16} , 6.18×10^{16} and 8.82×10^{17} cm^{-3}, respectively, named as S1, S2, S3 and S4, were also investigated for comparison and discussion. The thicknesses of all the Si-doped GaN epilayers were 4μm. The Raman scattering spectra of all the samples were measured under a backscattering geometric configuration with $z(x,x+y)\overline{z}$ (z direction aligns with the *c*-axis of crystal) using a WITec-Alpha confocal micro-Raman system at room temperature. The laser line of 514.5 nm of an argon gas laser with the output power of 30 mW was employed as the excitation light of Raman scattering measurements. X-ray diffraction (XRD) patterns of the samples were obtained by a Siemens D5000 X-ray diffractometer with an angle-scanning step of 0.005°.

Results and discussion

Figure 1 shows the measured Raman spectra of the Fe-doped samples and the reference bulk G2 as well as the control epilayer G1, where the two major Raman active modes, namely E_2^{high} and A_1(LO) (LO is an acronym of longitudinal optical phonon) peaks are illustrated. The E_2^{high} peak intensity of all the spectra is normalized, and the spectra are shifted vertically for clarity.

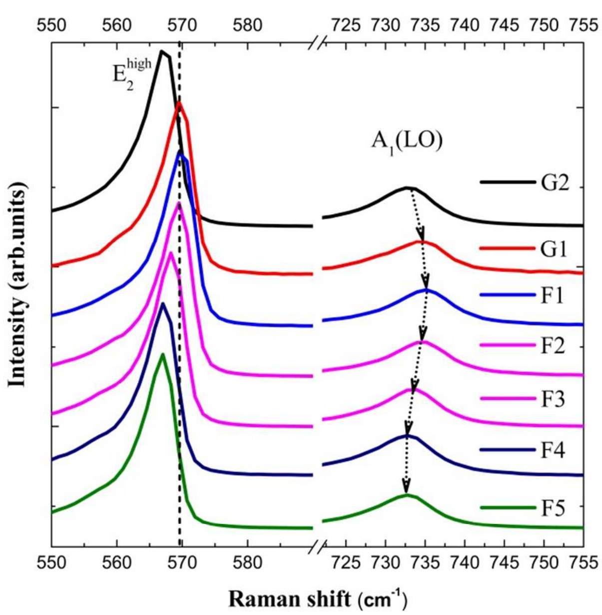

Fig. 1 Measured micro-Raman scattering spectra of the Fe-doped GaN epilayers. The spectra of samples G1 and G2 are also illustrated for comparison. The spectra were normalized at E_2^{high} peak and shifted vertically for clarification. The vertical dashed line and the short dotted arrows are drawn to guide the eyes.

The E_2^{high} mode of GaN epilayers is proved to be sensitive to the variation of strain in the films.[7, 16] From Fig. 1, it can be seen that the peak position (566.83cm^{-1}) of the E_2^{high} mode of the free-standing GaN thick layer (G2) is very close to the reported strain-free value of 566.2cm^{-1}, indicating that the residual strain inside it is nearly completely released.[17-19] In all the remaining GaN epilayers grown on sapphire, however, compressive strain presents, verified by the observed blue-shift of the E_2^{high} mode with respect to the almost strain free sample G2. For example, the E_2^{high} mode of the sample G1 located at 569.49cm^{-1}, which is evidently higher than that of the free-standing sample. Interestingly, the E_2^{high} peaks of the Fe-doped GaN epilayers shift towards the lower frequency direction as the Fe doping concentration increases, suggesting that the compressive strain in the epilayers tends to relax with increasing the doping concentration. The A_1(LO) peaks also shift towards the lower energy direction. However, due to the strong A_1(LO)-plasmon coupling, the redshift of A_1(LO) with the increase of Fe doing concentration has to be carefully discussed in late section. In sharp contrast to the case of Fe-doped samples, the Si-doped GaN epilayers grown on sapphire show different behaviors, as depicted in Fig. 2.

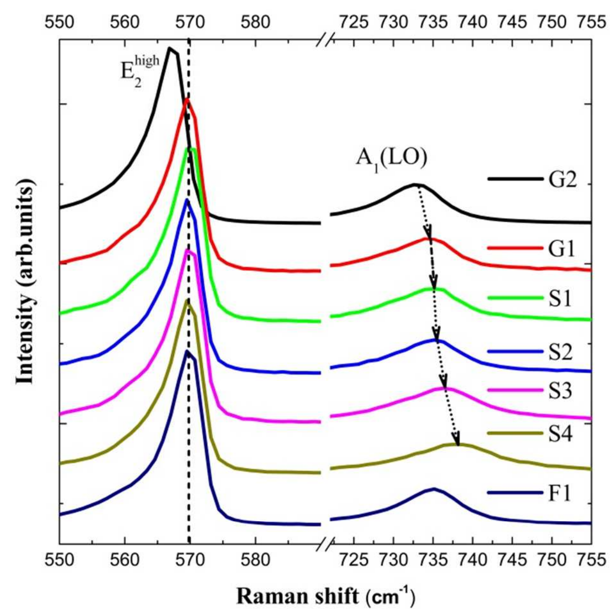

Fig. 2 Measured Raman spectra of Si-doped GaN epilayers. Results from G1, G2 and F1 are also included for comparison. The spectra were normalized at E_2^{high} peak and shifted vertically for clarification. The vertical dashed line and the short dotted arrows are drawn to guide the eyes.

The E_2^{high} peaks of these Si-doped samples (S1, S2, S3 and S4) do not show any observable shift, compared with the intentionally undoped GaN epilayer (i.e., sample G1). However, their A_1(LO) peaks move towards the higher energy side as the Si doping concentration increases. As argued earlier, the E_2^{high} mode is more sensitive to the variation of biaxial strain in the GaN epilayers. It should be noted that the incorporation of foreign atoms into GaN can introduce a hydrostatic strain.[14, 17] At particular, it is expected to be considerable at high dopant concentrations. In the Si-doped

GaN epilayers studied in the present work, no observable shift is observed for the E_2^{high} mode, suggesting that the residual strain shows no observable change with increasing the Si doping concentration at least in the interested range, i.e., < 9×10^{17} cm^{-3}. Nevertheless, we would like to mention that for the Si-doped GaN epilayers with higher doping concentrations, the relaxation tendency of the compressive strain was observed by Lee *et al*,[11] although they did not discuss the A_1(LO) mode behavior in their work. For the Si-doped samples studied in the present work, the Si doping has been shown to significantly influence the electron concentration due to the incorporation of Si atoms in GaN.[20] We thus looked for other mechanism such as LO phonon-electronic plasmon coupling to interpret the observed blueshift of the A_1(LO) mode in the Si-doped epilayers.[21-25] Here it is worth noting that from the two prominent Raman features (E_2^{high} and A_1(LO)) of the Fe- and Si-doped GaN epilayers, we can observe that no significant degradation in crystalline quality is caused by incorporation of foreign doping atoms. This point is also supported by the XRD results shown later.

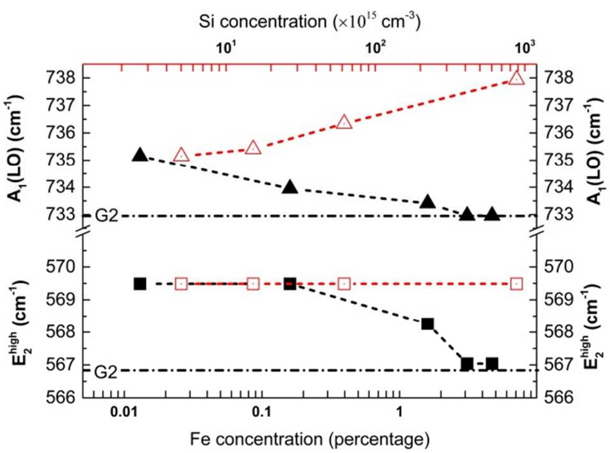

Fig. 3 E_2^{high} and A_1(LO) peak position change of Fe-doped and Si-doped GaN epilayers. E_2^{high} peak positions are represented by squares, solid for Fe-doped ones, empty for Si-doped ones. A_1(LO) peak positions are represented by triangles, solid for Fe-doped ones, empty for Si-doped ones. Scatters are connected by dashed lines for guidance. The two horizontal dash-dotted lines mark the positions of E_2^{high} and A_1(LO) peaks of the free-standing layer G2, respectively.

For a clear comparison, the peak positions of E_2^{high} and A_1(LO) modes directly extracted from the measured spectra in Figs. 1 and 2 are summarized in Fig. 3. The two dash-dotted lines are drawn to mark the positions of E_2^{high} and A_1(LO) peaks of the free-standing sample G2. It is quite clear that both the E_2^{high} (solid squares) and A_1(LO) (solid triangles) modes of the Fe-doped samples exhibit noticeable redshift with an increase in the doping concentration, and finally get close to the corresponding peak positions of the free-standing sample G2. Nevertheless, for the Si doped samples, the A_1(LO) peak position displays a blueshift while the E_2^{high} peak does not show any observable shift with an increase in the Si concentration.

Before we discuss the details of A_1(LO) mode, we would like to point out that the reduction of the biaxial strain in the Fe-doped epilayers may influence the peak position of A_1(LO) mode, although the E_2^{high} has already shown to be more sensitive to the variation of biaxial strain in the epilayers.[16, 26] It should be mentioned that similar pressure coefficients were reported for E_2^{high} and A_1(LO) modes under external hydrostatic[19] or uniaxial pressure.[27] For the Si-doped GaN samples, the observed blueshift of A_1(LO) mode can be well interpreted with the LO phonon-plasmon coupled mode since the E_2^{high} mode does not show any observable shift.

As mentioned earlier, a LO phonon-plasmon coupled model was adopted to simulate the broadening A_1(LO) peak (the upper branch of the LO phonon-plasmon coupled mode) in the Raman spectra.[9, 21, 22] The plasmon damping constant γ, phonon damping constant Γ, and plasmon frequency ω_p were treated as the fitting parameters in the model. It has been previously demonstrated that the A_1(LO) peak position was mainly determined by the plasmon frequency and damping constant while its peak intensity was primarily affected by the phonon damping.[21] Even if considering the shift of A_1(LO) peak partially caused by the change of residual strain in Fe-doped samples (i.e., 30% contribution), the fitting results still demonstrate a clear reduction of carrier concentration as increasing Fe doping. The values for the frequencies of TO (transverse optical mode) and LO phonons in GaN used in the fitting process were 530.85 and 732.95 cm^{-1}, respectively, which were taken directly from the Raman spectra of the free-standing sample G2 (A_1(TO) and A_1(LO) modes, respectively, details not shown here). The plasmon frequency ω_p was used to derive the carrier concentration by the relation (in cgs units)

$$\omega_p^2 = \frac{4\pi n e^2}{\varepsilon_\infty m_e^*}, \qquad (1)$$

where ε_∞ is the optical dielectric constant, m_e^* is the electron effective mass, and n is free carrier concentration. For the Si-doped samples, ω_p is found to increase with raising the dopant concentration. For example, ω_p=63 cm^{-1} for S1, and 159 cm^{-1} for S4, are in good agreement with the reported results.[9] For the intentionally undoped epilayer G1, ω_p is found to be 61cm^{-1}, which indicates the n-type nature of as-grown GaN epilayers.[9, 22] On the contrary, ω_p strongly decreases with increasing the Fe concentration in the Fe-doped samples, i.e., 120 cm^{-1} for F1, ~2.4 cm^{-1} for F4 and F5, showing that Fe dopants in GaN can act as efficient "electron killers" for realizing semi-insulating GaN.[3, 4] Neutron irradiation was also observed to produce similar effect.[22] Figure 4 shows the fitting curves (solid lines) and experimental spectra (lines + symbols) of samples F1 and F4. A good agreement between theory and experiment is achieved, as seen in Fig. 4.

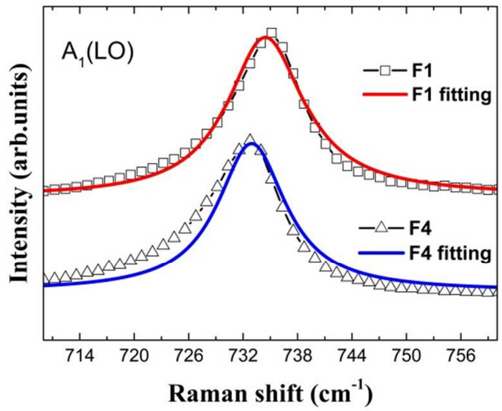

Fig. 4 Fitting curves (solid lines) of A_1(LO) mode of samples F1 and F4 by the LO phonon-plasmon coupling model. The respective experimental results are represented by empty squares and triangles connected by lines for F1 and F4, respectively.

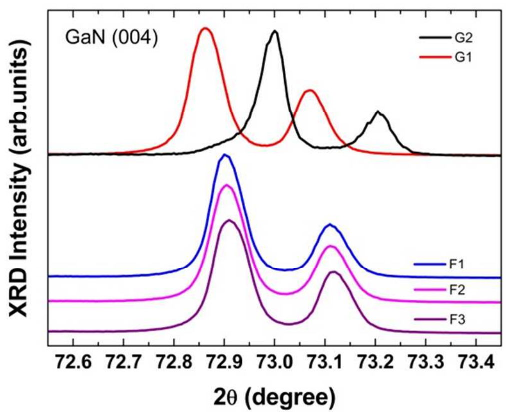

Fig. 5 XRD 2θ scanning patterns of the Fe-doped samples F1, F2 and F3. The XRD results from sample G1 and G2 are also depicted in the upper part for comparison. Note that only the diffraction patterns from the GaN (004) plane were shown. The double peak structure is due to the diffractions of Cu Kα1 and Kα2 lines by GaN (004) plane. The XRD curves of the Fe-doped samples were shifted vertically for clarity.

Now we return to discuss the E_2^{high} mode and strain in more details. As seen in Fig. 1 and 3, the E_2^{high} peak does not show observable shift when the Fe doping concentration is low. However, noticeable redshift is clearly observed when the doping concentration becomes larger. If a theoretical stress coefficient of 2.56 cm^{-1}/GPa is adopted for the E_2^{high} mode of GaN epilayer grown on sapphire,[7, 23] the stresses of the Fe-doped samples F1, F2, F3, F4 and F5 are found to be 1.040, 1.040, 0.560, 0.082 and 0.082 GPa, respectively. Obviously, the stresses in the Fe doped GaN epilayers tend to reduce as the Fe doping concentration increases. Like other foreign atoms, the incorporation of Fe atoms into GaN may induce an additional hydrostatic strain via producing point defects.[17] If Fe atoms are present in GaN as interstitials, they may bring out a tensile hydrostatic strain. If they exist as the substitutions of Ga, a compressive hydrostatic strain could be introduced due to the smaller atomic radius of Fe. We believe that Fe atoms could exist in GaN in the two geometric configurations. However, as the Fe doping concentration increases, the percentage of interstitial Fe atoms may increase and thus leads to the partial relaxation of the compressive residual strain in the GaN films.

In order to obtain further evidence of relaxation of the residual strain in the Fe-doped GaN epilayers, XRD measurements were performed on the samples. Figure 5 shows the measured XRD 2θ scanning patterns of G2, G1, F1, F2 and F3. The double peak structure originates from the diffractions of Cu Kα1 ($\lambda = 1.5406\,\mathring{A}$) and Kα2 lines by the GaN (004) plane. The (004) 2θ peak from the sapphire substrate (52.553^0, PDF Pattern no 10-0173) was used to calibrate the peak positions of G1, F1, F2 and F3. The XRD data of sample F4 and F5 are not shown here because the diffraction signals from their sapphire substrates were not detected, which could be due to the limited penetration depth of X-ray because the thicknesses of Fe-doped epilayers in these sample are quite large. Directly read out from Fig. 5, the GaN (004) 2θ peak position of the free-standing sample (G2) is 73°, which is the same as the standard data (73.000°, PDF Pattern no 02-1078, with a_0=3.18600Å and c_0=5.17800Å). Double-peak fitting was performed to determine the (004) 2θ peak positions of the rest XRD curves using Loretzian lineshape function. Bragg's law ($2d \times \sin\theta = n\lambda$, here n=4) was used to calculate the lattice parameter c of these samples, and then obtained lattice parameters were used to compute the residual strain along the c-axis with the equation: $\varepsilon_{zz} = (c - c_0)/c_0$. The results are summarized in Table I.

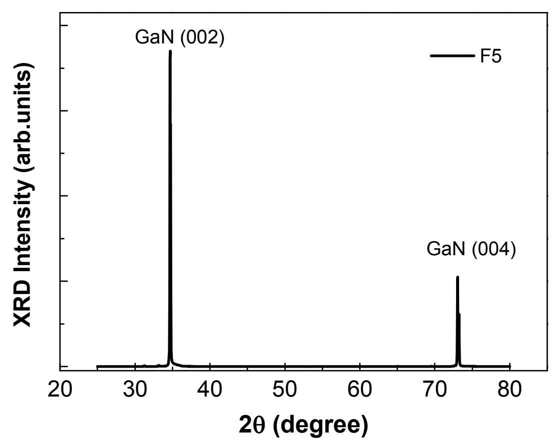

Fig. 6 XRD 2θ scanning patterns of sample F5 with the highest Fe doping concentration in a wide scanning range of 25-80 degrees. The dominant sharp diffraction peaks from GaN (002) and (004) planes indicate that the sample remains good wurtzite structure.

Clearly, the strain ε_{zz} of the epilayers reduces as the Fe concentration increases, which is consistent with the Raman results discussed earlier. It should be noted that even for the GaN film with the highest Fe doping concentration such as sample F5 studied in this work, it still holds good wurtzite lattice structure, as shown in Fig. 6.

Table I. 2θ values in the XRD measurements obtained from the double-peak fitting and residual strain along *c*-axis calculated based on them in samples G1, F1, F2 and F3. The values of the free-standing sample G2 are also listed for comparison.

Sample	G1	F1	F2	F3	G2
2θ (degree)	72.86428 $\pm 2.9\times 10^{-4}$	72.90455 $\pm 2.8\times 10^{-4}$	72.90648 $\pm 3.1\times 10^{-4}$	72.91265 $\pm 3.5\times 10^{-4}$	73
ε_{zz} (%)	0.200	0.152	0.150	0.142	0

At last, we would like to point out that all the experimental data, no matter whether from the Raman spectra or XRD patterns, reflect the average information of respective quantities over a certain thickness. It has been experimentally shown that vertical gradients in strain as well as carrier concentration can occur in thick GaN layers grown on sapphire, especially within about a few microns from the sapphire/GaN interface.[28] For the Fe-doped samples studied here, their thicknesses are larger than 20μm. Therefore, the Raman and XRD data from these samples carry the average information of the Fe-doped epilayer in the vertical range far from the sapphire/GaN interface.

Conclusions

In conclusion, Fe doping was demonstrated to have significant impact not only on the background electron concentration but also on the residual strain in the GaN epilayers grown on sapphire through analyzing the micro-Raman spectra and XRD patterns. In sharp contrast to the case of Si doping, the compensation of Fe doping to the background electron concentration is likely efficient when the concentration is relatively low. More interestingly, as the Fe doping concentration increases its effect on the relaxation of the compressive residual strain of the GaN epilayers grown on sapphire becomes significant. These findings show that Fe doping may provide a possible method for engineering the strain of GaN heteroepilayers.

Acknowledgements

This work was supported by HK RGC-GRF Grants (No. HKU 703612P) and Shenzhen Municipal Science and Technology Innovation Council (Contract No. JCYJ20120615142933076). C. C. Zheng acknowledges the support from XJTLU by RDF-12-02-03 and the English language proof reading by S. Hartigan from Language Centre.

Notes and references

[a] Mathematics and Physics Centre, Xi'an Jiaotong-Liverpool University, Suzhou 215123, China.

[b] Department of Physics, HKU-Shenzhen Institute of Research and Innovation (HKU-SIRI), and HKU-CAS Joint Laboratory on New Materials, The University of Hong Kong, Pokfulam Road, Hong Kong, China. Email: sjxu@hku.hk; Fax: +852 25599152; Tel: +852 22415636

[c] Suzhou Institute of Nano-Tech and Nano-Bionics, Chinese Academy of Sciences, Suzhou 215123, China.

[d] State Key Laboratory on Integrated Optoelectronics, Institute of Semiconductors, Chinese Academy of Sciences, Beijing 100083, China.

[†] Present address: School of Science, Beijing University of Posts and Telecommunications, Beijing 100876, China.

Electronic Supplementary Information (ESI) available: [details of any supplementary information available should be included here]. See DOI: 10.1039/b000000x/

1 A. H. Morkoc, Nitride Semiconductors and Devices. (Springer, Berlin, 1999).
2 S. Nakamura, G. Fasol, and S. J. Pearton, The Blue Laser Diodes. (Springer, Berlin, 2000).
3 S. Heikman, S. Keller, S. P. DenBaars, and U. K. Mishra, *Appl. Phys. Lett.* 2002, **81**, 439.
4 A. Y. Polyakov, N. B. Smirnov, A. V. Govorkov, and S. J. Pearton, *Appl. Phys. Lett.* 2003, **83**, 3314.
5 W. Lee, J.-H. Ryou, D. Yoo, J. Limb, R. D. Dupuis, D. Hanser, E. Preble, N. M. Williams, and K. Evans, *Appl. Phys. Lett.* 2007, **90**, 093509.
6 G. M. Dalpian, J. L. Da Silva, and S.-H. Wei, *Phys. Rev. B* 2009, **79**, 241201.
7 D. G. Zhao, S. J. Xu, M. H. Xie, S. Y. Tong, and H. Yang, *Appl. Phys. Lett.* 2003, **83**, 677.
8 C. C. Zheng, S. J. Xu, J. Q. Ning, W. Bao, J. F. Wang, J. Gao, J. M. Liu, J. H. Zhu, and X. L. Liu, *Semicond. Sci. Technol.* 2012, **27**, 035008.
9 T. Kozawa, T. Kachi, H. Kano, Y. Taga, M. Hashimoto, N. Koide, and K. Manabe, *J. Appl. Phys.* 1994, **75**, 1098.
10 H. Harima, H. Sakashita, T. Inoue, and S.-I. Nakashima, *J. Cryst. Growth* 1998, **189**, 672.
11 I.-H. Lee, I.-H. Choi, C.-R. Lee, E.-J. Shin, D. Kim, S.K. Noh, S.-J. Son, K. Y. Lim, and H. J. Lee, *J. Appl. Phys.* 1998, **83**, 5787.
12 M. H. Kane, S. Gupta, W. E. Fenwick, N. Li, E. H. Park, M. Strassburg, and I. T. Ferguson, *Phys. Status Solidi A* 2007, **204**, 61.
13 Z. K. Tao, R. Zhang, X. G. Cui, X. Q. Xiu, G. Y. Zhang, Z. L. Xie, S. L. Gu, Y. Shi, and Y. D. Zheng, *Chin. Phys. Lett.* 2008, **25**, 1476.
14 M. Katsikini, F. Pinakidou, J. Arvanitidis, E. C. Paloura, S. Ves, Ph. Komninou, Z. Bougrioua, E. Iliopoulos, and T. D. Moustakas, *Mater. Sci. Eng. B* 2011, **176**, 723.
15 E. Malguth, A. Hoffmann, W. Gehlhoff, O. Gelhausen, M. R. Philips, and X. Xu, *Phys. Rev. B* 2006, **74**, 165202.
16 F. Demangeot, J. Frandon, M. A. Renucci, O. Briot, B. Gil and R. L. Aulombard, *Solid State Commun.* 1996, **100**, 207.
17 C. Kisielowski, J. Krüger, S. Ruvimov, T. Suski, J. W. Ager III, E. Jones, Z. Liliental-Weber, M. Rubin, E. R. Weber, M. D. Bremser, and R. F. Davis, *Phys. Rev. B* 1996, **54**, 17745.
18 V. Darakchieva, T. Paskova, P. P. Paskov, B. Monemar, N. Ashkenov, and M. Schubert, *Phys. Status Solid. A* 2003, **195**, 516.
19 A. R. Goni, H. Siegle, K. Syassen, C. Thomsen, and J.-M. Wagner, *Phys. Rev. B* 2001, **64**, 035205.
20 C. C. Zheng, S. J. Xu, F. Zhang, J. Q. Ning, D. G. Zhao, H. Yang, and C. M. Che, *Appl. Phys. Lett.* 2012, **101**, 191102.
21 H. Harima, S. I. Nakashima, and T. Uemura, *J. Appl. Phys.* 1995, **78**, 1996.

22 R. X. Wang, S. J. Xu, S. Fung, C. C. Beling, K. Wang, S. Li, Z. F. Wei, T. J. Zhou, J. D. Zhang, and Y. Huang, *Appl. Phys. Lett.* 2005, **87**, 031906.
23 J.-M. Wagner and F. Bechstedt, *Appl. Phys. Lett.* 2000, **77**, 346.
24 C. Wetzel, A. L. Chen, T. Suski, J. W. Ager III, and W. Walukiewicz, Phys. Stat. Sol. (b) 1996, **198**, 243.
25 L. Bergman, M. Dutta, R. J. Nemanich, in Raman scattering in Materials Science, Eds. by W. H. Weber and R. Merlin, (Springer-Verlag Berlin Heidelberg,2000), Chap. 7, pp. 296.
26 J.-Y. Lu, D.-M. Deng, Y. Wang, K. J. Chen, K.-M. Lau, and T.-Y. Zhang, *AIP Adv.* 2011, **1**, 032132.
27 G. Callsen, J. S. Reparaz, M. R. Wagner, R. Kirste, C. Nenstiel, A. Hoffmann, and M. R. Phillips, *Appl. Phys. Lett.* 2011, **98**, 061906.
28 H. Siegle, A. Hoffmann, L. Eckey, C. Thomsen, J. Christen, F. Bertram, D. Schmidt, D. Rudloff, and K. Hiramatsu, *Appl. Phys. Lett.* 1997, **71**, 2490.